



This is a repository copy of *A cytostatic ruthenium(II)-platinum(II) bis(terpyridyl) anticancer complex that blocks entry into S phase by up-regulating p27KIP1.*

White Rose Research Online URL for this paper:
<http://eprints.whiterose.ac.uk/85831/>

Version: Accepted Version

Article:

Ramu, V., Gill, M.R., Jarman, P.J. et al. (4 more authors) (2015) A cytostatic ruthenium(II)-platinum(II) bis(terpyridyl) anticancer complex that blocks entry into S phase by up-regulating p27KIP1. *Chemistry - A European Journal*, 21 (25). pp. 9185-9197. ISSN 0947-6539

<https://doi.org/10.1002/chem.201500561>

Reuse

Unless indicated otherwise, fulltext items are protected by copyright with all rights reserved. The copyright exception in section 29 of the Copyright, Designs and Patents Act 1988 allows the making of a single copy solely for the purpose of non-commercial research or private study within the limits of fair dealing. The publisher or other rights-holder may allow further reproduction and re-use of this version - refer to the White Rose Research Online record for this item. Where records identify the publisher as the copyright holder, users can verify any specific terms of use on the publisher's website.

Takedown

If you consider content in White Rose Research Online to be in breach of UK law, please notify us by emailing eprints@whiterose.ac.uk including the URL of the record and the reason for the withdrawal request.



eprints@whiterose.ac.uk
<https://eprints.whiterose.ac.uk/>

A cytostatic ruthenium(II)-platinum(II) bis(terpyridyl) anticancer complex that blocks entry into S phase by up-regulating p27^{KIP1}

Vadde Ramu,^{[a]†} Martin R. Gill,^{[b]†} Paul Jarman,^[c] David Turton,^[b] Jim A. Thomas,^{[c]*} Amitava Das^{[a]*} and Carl Smythe^{[b]*}

^[a]Organic Chemistry Division, CSIR-National Chemical Laboratory, Pune, 411008, Maharashtra, India.

^[b]Department of Biomedical Science, University of Sheffield, UK.

^[c]Department of Chemistry, University of Sheffield, UK.

†These authors contributed equally to this work.

*E-mail: c.g.w.smythe@sheffield.ac.uk. Fax: +44 (0)114 222 2787; Tel: +44 (0)114 222 4643; a.das@ncl.res.in. Fax: +91 (0)20-2590262; Tel: +91 (0)20-25902385. james.thomas@sheffield.ac.uk. Fax: +44 (0)114 22 29436; Tel: +44 (0)114 22 29325.

Abstract: Cytostatic agents that interfere with specific cellular components to prevent cancer cell growth offer an attractive alternative, or complement, to traditional cytotoxic chemotherapy. Here, we describe the synthesis and characterization of a new binuclear Ru^{II}-Pt^{II} complex [Ru(tpy)(tpypma)Pt(Cl)(DMSO)]³⁺ (tpy = 2,2':6',2''-terpyridine and tpypma = 4-([2,2':6',2''-terpyridine]-4'-yl)-N-(pyridin-2-ylmethyl)aniline), VR54, which employs the extended terpyridine tpypma ligand to link the two metal centres. VR54 binds DNA *in vitro* by non-intercalative reversible mechanisms ($K_b = 1.3 \times 10^5 \text{ M}^{-1}$) and does not irreversibly bind guanosine. Cellular studies reveal VR54 suppresses proliferation of A2780 ovarian cancer cells with no cross-resistance in the A2780CIS cisplatin-resistant cell line. Through the preparation of mononuclear Ru^{II} and Pt^{II} structural derivatives we determine both metal centres are required for this anti-proliferative activity. In stark contrast to cisplatin, VR54 does not activate the DNA damage response network nor induces significant levels of cell death. Instead, VR54 is cytostatic and inhibits cell proliferation by up-regulating the cyclin-dependent kinase inhibitor p27^{KIP1} and inhibition of Rb phosphorylation; which blocks entry into S phase and results in G1 cell cycle arrest. Thus, VR54 inhibits cancer cell growth via a gain of function at the G1 restriction point. This is the first metal coordination compound to demonstrate such activity.

Introduction

Based on the success of cisplatin, platinum-based drugs remain the first line of treatment - either alone or in combination with other anticancer drugs - for a variety of cancers, including head and neck, testicular and ovarian.^[1] One of the targets of cisplatin is DNA, where - following ligand substitution - the molecule binds irreversibly to the nucleobases, typically at N₇ sites of guanine, creating both intra and inter-strand cross-links.^[2] Since the cellular DNA mismatch repair or nucleotide excision repair systems do not process these lesions efficiently, an apoptotic

cell death response is induced.^[3] Despite the success of cisplatin, intrinsic or acquired drug resistance combined with toxicity represents a significant challenge for the future of platinum chemotherapy.^[4] Mechanisms that contribute to platinum-based resistance include changes in efficiency of drug accumulation, intra-cellular thiol levels and DNA adduct repair,^[4] with resistance often being multifactorial. Such resistance requires ever-greater doses of platinum therapeutic, eventually precluding safe use of the drug due to the inherent high toxicity of the molecule.

One strategy to overcome this problem has involved the design of new transition metal-based compounds, which aim to utilise the opportunities afforded by co-ordination chemistry to explore novel chemical space in cancer biology. Specifically, by employing a variety of metal centres, the effect of ancillary and active ligand(s) on reactivity, cellular uptake and anti-proliferative potency has been explored in detail.^[5] With some exceptions,^[6] work in this area has often focussed on the development of potent, purely cytotoxic systems. However, clinical application of cytotoxic drugs is often restricted by narrow therapeutic windows and inherent off-target tissue toxicity.^[7] This principle may be illustrated by platinum-based drugs themselves: carboplatin, a less potent cisplatin-derivative, was introduced in an attempt to reduce the nephrotoxicity and emetic properties of the parent complex,^[1] while clinical trials of the highly cytotoxic trisplatinum agent BBR 3464 ceased due to its severe dose-limiting side-effects.^[8]

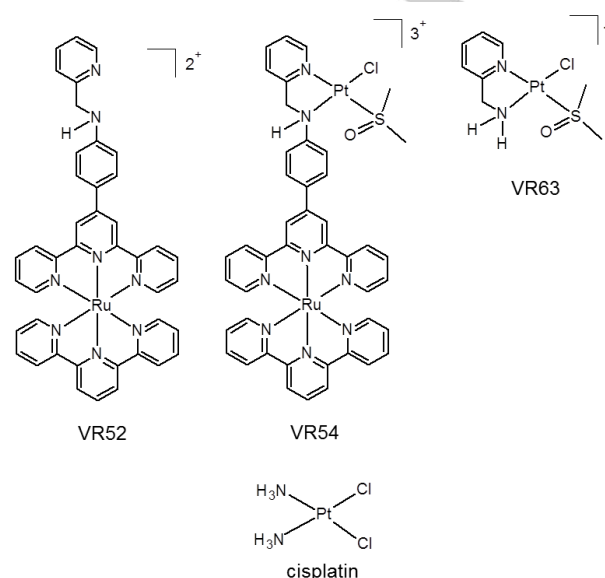
As insights into the cell biology of cancer have developed, targeted therapy has emerged as an alternative approach to conventional cytotoxic chemotherapy.^[9] Utilising a detailed understanding of the molecular aetiology of individual tumours, targeted therapies aim to inhibit the growth and spread of cancer either by selectively down-regulating intra-cellular pathways on which specific cancers have become dependent,^[10] and /or by re-activating tumour-suppressor pathways that have been down-regulated in a tumour.^[11]

Much current targeted therapy development has focused on use of cytostatic therapeutics^[12] to halt cell proliferation by modulating molecular components, currently most often growth factor receptors, involved in cell cycle progression and consequently proliferation. Targeted therapeutics include, but are not restricted to, signal transduction inhibitors that interfere with the transition from G1 to S phase, blocking cellular signalling pathways that regulate this cell cycle progression known as the restriction point. The normal function of the restriction point is to ensure that, in the absence of appropriate extra-cellular proliferative cues, the cyclin-dependent kinase cyclin D/Cdk4 is not activated, preventing cell cycle progression and proliferation.^[13] An example of a clinically relevant targeted therapeutic is the monoclonal antibody trastuzumab (Herceptin), which suppresses growth of relevant (Her2⁺) human breast cancers by interfering with the receptor tyrosine kinase HER2.^[14] Further clinical examples include the combinational therapy drug Lapatinib (Tyverb, GW572016), a dual inhibitor of the epidermal growth factor (EGF) and HER2 receptor tyrosine kinases^[15], as well as the small molecule Tamoxifen which, in active form, antagonises the activation of estrogen receptors (ER) by estrogen in ER-positive breast cancer cells.^[15a, 16] Tamoxifen is a very effective primary treatment, in pre- and post-menopausal women, as well as in the metastatic setting for tumours that express the estrogen receptor,^[17] despite the fact that in relevant cells it is not especially potent, with a reported half inhibitory concentration, IC₅₀, of 27 μM.^[18]

In all cases, these therapeutic approaches have the effect of preventing cyclin D/Cdk4 activation to bring about cytostatic G1 arrest. However, therapeutic efficacy in prevention of cyclin D/Cdk4 activation requires significant levels of the cyclin-dependent kinase inhibitor, p27^{KIP1},^[19] a tumour suppressor that binds to and inactivates the kinase. While not mutated in cancer, p27^{KIP1} levels are frequently down-regulated in multiple cancer types.^[13] Clearly then, there is significant unmet need for novel therapeutics that up-regulate p27^{KIP1} function to induce growth arrest in human cancers, not least where the targeted therapeutics above are clinically indicated,^[15a, 16] but potentially also where signal transduction targets have yet to be identified, as in so-called "triple-negative" breast and ovarian cancers.^[20]

Herein, we report the synthesis, DNA-binding properties, and anticancer activity of a new Ru^{II}-Pt^{II} binuclear terpyridine-derived complex, VR54 (Scheme 1), where the ditopic ligand tpy_{pma} (tpypma = 4-([2,2':6',2''-terpyridine]-4'-yl)-N-(pyridin-2-ylmethyl)aniline) allows an octahedral ruthenium(II) terpyridyl centre to be linked to a Pt^{II} moiety. We show that VR54 halts the growth of human ovarian cell lines and, importantly, sensitivity to the compound is retained in cisplatin-resistant cells. Through comparison with the mononuclear Ru^{II} and Pt^{II} compounds VR52 and VR63 (Scheme 1), we establish that both metal centres of VR54 are required for bioactivity. Systematic analyses at the molecular and cellular level show that, unlike conventional platinum therapeutics, VR54 does not co-ordinate with the nucleobase guanosine, and consequently does not generate a cytotoxic response or pro-apoptotic signals via the activation of the DNA damage response network. Instead VR54 acts by up-regulating the Cdk inhibitor p27^{KIP1}, leading to hypo-

phosphorylation of Rb and thereby blocking cell-cycle progression from G1 to S phase.



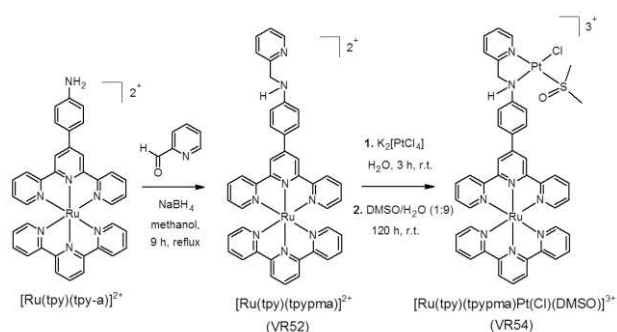
Scheme 1. Structures of complexes used in this study.

Results

Synthesis and characterization

The monometallic Ru^{II} complex VR52 and bimetallic Ru^{II}-Pt^{II} polypyridyl complex VR54 were synthesized through the route shown in Scheme 2. This synthetic pathway involves the preparation of the precursor complex [Ru(tpy)(tpy-a)]²⁺ (tpy = 2,2':6',2''-terpyridine; tpy-a = 4-([2,2':6',2''-terpyridine]-4-yl)-aniline),^[21] followed by conversion of tpy-a to the ditopic ligand tpy_{pma}, generating the mononuclear Ru^{II} complex [Ru(tpy)(tpypma)]²⁺ (VR52). Complex VR52 was then reacted with K₂PtCl₄ to obtain the bimetallic Ru^{II}-Pt^{II} intermediate complex [Ru(tpy)(tpypma)Pt(Cl)₂]²⁺ (VR53). We initially wished to include VR53 within our biological studies for comparative purposes, however the complex displays very poor aqueous solubility; full dissolution only occurs following exchange of a chloride ligand in water or other coordinating solvents. Accordingly, this intermediate complex was reacted with DMSO to yield the more soluble tricationic complex [Ru(tpy)(tpypma)Pt(Cl)(DMSO)]³⁺ (VR54). The mononuclear Pt^{II} compound [Pt(amp)(Cl)(DMSO)]⁺ (amp = 2-pyridylmethylamine) (VR63) was prepared in an analogous fashion from the previously-reported precursor [Pt(amp)(Cl)₂].^[22] Full characterization of VR52, VR54 and VR63 using standard spectroscopic and analytical techniques is included within the experimental section and Figures S1-S10 in the Supporting Information. The addition of a single DMSO ligand to the Pt^{II} centre for both VR54 and VR63 is consistent with elemental analysis and mass spectroscopy. IR and ¹⁹⁵Pt NMR spectra confirm the proposed chemical structures: For VR54, the IR

spectrum reveals a broad band in the region at 1029 – 1100 cm^{-1} ; a $\nu(\text{SO})$ stretching frequency indicative of a sulfur-coordinated DMSO,^[23] while the single ^{195}Pt resonance observed at -2967 ppm is in good agreement with structurally related Pt^{II} compounds.^[24] Likewise for VR63, a single ^{195}Pt resonance is observed at -3142 ppm. Based on trans effects, we assign the DMSO ligand to the trans-position with respects to the pyridin-2-yl-methyl coordination site of the tppma or amp ligands for VR54 and VR63 respectively. The UV-visible absorption spectra of VR52, VR54 and VR63 are summarized in Table 1. Through comparison with related molecules,^[21] bands centred at approximately 273 nm and 309 nm for complexes VR52 and VR54 were assigned to intra- and inter-ligand electronic transitions. The visible region is dominated by broad ($\text{Ru}(\text{d}\pi) \rightarrow \text{tpy}/\text{tppma}(\pi^*)$ -based $^1\text{MLCT}$ (metal-to-ligand charge transfer) bands centred at 492 nm ($\epsilon = 19170 \text{ M}^{-1} \text{ cm}^{-1}$) and 489 nm ($\epsilon = 15750 \text{ M}^{-1} \text{ cm}^{-1}$) for complexes VR52 and VR54 respectively, which are responsible for the deep red colour of each ruthenium complex. Complex VR63 has one absorption band in the UV region centred at 274 nm ($\epsilon = \text{ca. } 5,100 \text{ M}^{-1} \text{ cm}^{-1}$), corresponding to aromatic intra-ligand electronic transitions. As is common for $\text{Ru}(\text{tpy})_2$ derivatives,^[25] VR52 and VR54 demonstrated negligible luminescence upon MLCT excitation and are virtually non-emissive.



Scheme 2. Synthesis of VR52 and VR54.

Table 1. Photophysical data for VR52, VR54 and VR63.^[a]

Complex	$\lambda_{\text{abs}}/\text{nm}$ ($\epsilon / 10^3 \text{ M}^{-1} \text{ cm}^{-1}$)
VR52	273 (28.78), 309 (52.13), 492 (19.17)
VR54	272 (29.85), 308 (46.04), 489 (15.75)
VR63	274 (5.10)

[a] Recorded in acetonitrile at 298K.

DNA binding studies

Metal complexes have been widely studied for their ability to interact with DNA by either reversible or irreversible mechanisms.^[26] Furthermore, multiple modes of binding may be combined within one system. Indeed, several conjugate $\text{Ru}^{\text{II/III}}$ -

$\text{Pt}^{\text{II}}\text{Cl}_n$ complexes have been designed for this specific purpose.^[27] With these in mind, we characterized the interactions of VR52 and VR54 with DNA. The absorption spectra of VR52 and VR54 display distinctive changes in the presence of increasing concentrations of DNA, with both the $\pi \rightarrow \pi^*$ and MLCT absorption bands showing appreciable hypochromicity (Figures 1a,b). The changes in the MLCT band yield a typical saturation ligand-DNA binding curve (Figures 1a,b, insets) and higher binding ratios produced no additional changes in absorption spectra. Fits of these data to the McGhee von Hippel binding model^[28] reveal that both complexes have a similar affinity for DNA, with equilibrium binding constants, K_b , of $3.0 \times 10^5 \text{ M}^{-1}$ and $1.3 \times 10^5 \text{ M}^{-1}$ for VR52 and VR54 respectively. To determine DNA binding mode, relative specific viscosity of DNA was determined in the presence of increasing concentrations of each complex. The intercalator ethidium bromide and groove-binder $[\text{Ru}(\text{tpy})_2]^{2+}$ were used as controls for their respective modes of binding. In contrast to ethidium bromide, neither complex VR52 nor VR54 increased the relative viscosity of DNA solutions (Figure 1c), indicating that these complexes are not metallo-intercalators. This behaviour is consistent with previous reports on other extended Ru^{II} -terpyridyl complexes.^[29]

Cisplatin has previously been shown to possess a high affinity for guanine, where specifically the platinum(II) centre coordinates to the N_7 position after chloride ligand(s) substitution.^[2] Reactions with guanine derivatives such as guanosine are therefore commonly employed to assess whether platinum-containing drug candidates can bind DNA irreversibly.^[30] A structural comparison between VR54 and cisplatin suggest that the Ru^{II} - Pt^{II} complex could similarly react with DNA by way of direct coordination of the Pt^{II} metal centre to nucleobases. To explore this possibility, the extent of reaction of VR54 or cisplatin with solutions of guanosine in D_2O was followed by ^1H NMR spectroscopy. In order to assess the contribution, if any, of the Ru^{II} metal centre to Pt^{II} co-ordination, the reaction of the monometallic DMSO-substituted Pt^{II} complex VR63 with guanosine was included for comparison. As can be seen in Figure 2a, the addition of cisplatin to guanosine results in a decrease in the intensity of the H8 guanosine resonance at 8.10 ppm, accompanied by the appearance of two new resonance peaks at 8.51 and 8.63 ppm (Figure 2a), which increase in magnitude with exposure time. Likewise, a decrease in the H2 guanosine resonance at 5.95 ppm and corresponding appearance of the downfield-shifted peak at 6.10 ppm is observed (Figure 2a). This expected behaviour confirms that cisplatin binds guanosine via direct coordination (platination) of the Pt^{II} metal centre to the N_7 position of guanosine.^[30b] Similarly, addition of VR63 to guanosine resulted in rapid loss of H8 guanosine resonance and the appearance of two new resonance peaks at ~ 9.0 ppm, which is also consistent with the notion that VR63 interacts with this nucleobase via N_7 platination (Figure 2b).

In contrast to the behaviour demonstrated by cisplatin and VR63, no evidence of any effect on the NMR spectra of guanosine was observed following addition of VR54 (Figure 2c), indicating the Ru^{II} - Pt^{II} complex does not react with the nucleoside, behaviour comparable to the mononuclear Ru^{II}

complex VR52 (Figure S11). Taken together, this indicates that VR54 is highly unlikely to interact with DNA by irreversible binding following ligand substitution.

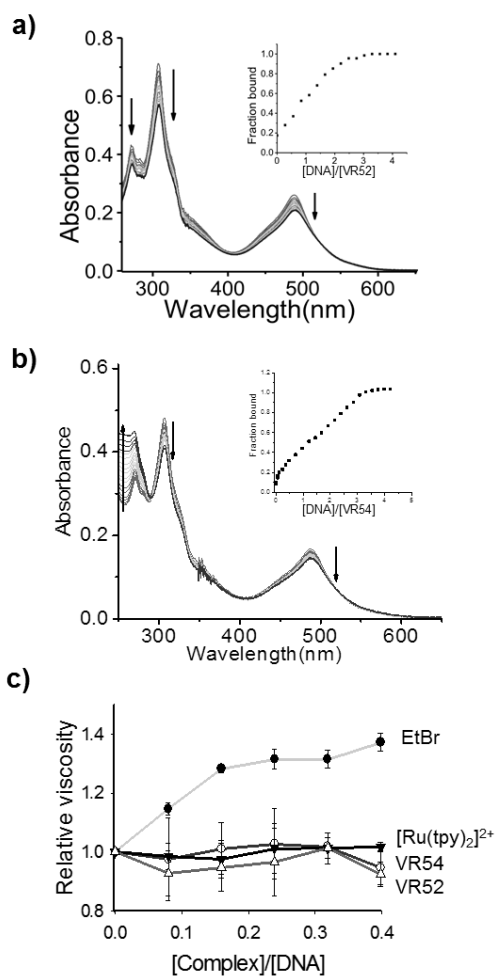


Figure 1. a, b) Changes in the UV-Vis absorbance spectra of VR52 (a) and VR54 (b) as a result of the addition of DNA, where hypochromicity is observed for each complex upon binding to DNA (indicated by arrows). Insets: Derived binding curves from hypochromicity data. c) Changes in the relative viscosity (η/η^0)^{1/3} of an aqueous DNA solution after addition of VR52 (○) or VR54 (△). The intercalator ethidium bromide (EtBr) and groove-binder [Ru(tpy)₂]²⁺ are included for comparative purposes. Studies carried out in 5 mM Tris-HCl, 25 mM NaCl, pH 7.2, 0.5% DMSO buffer.

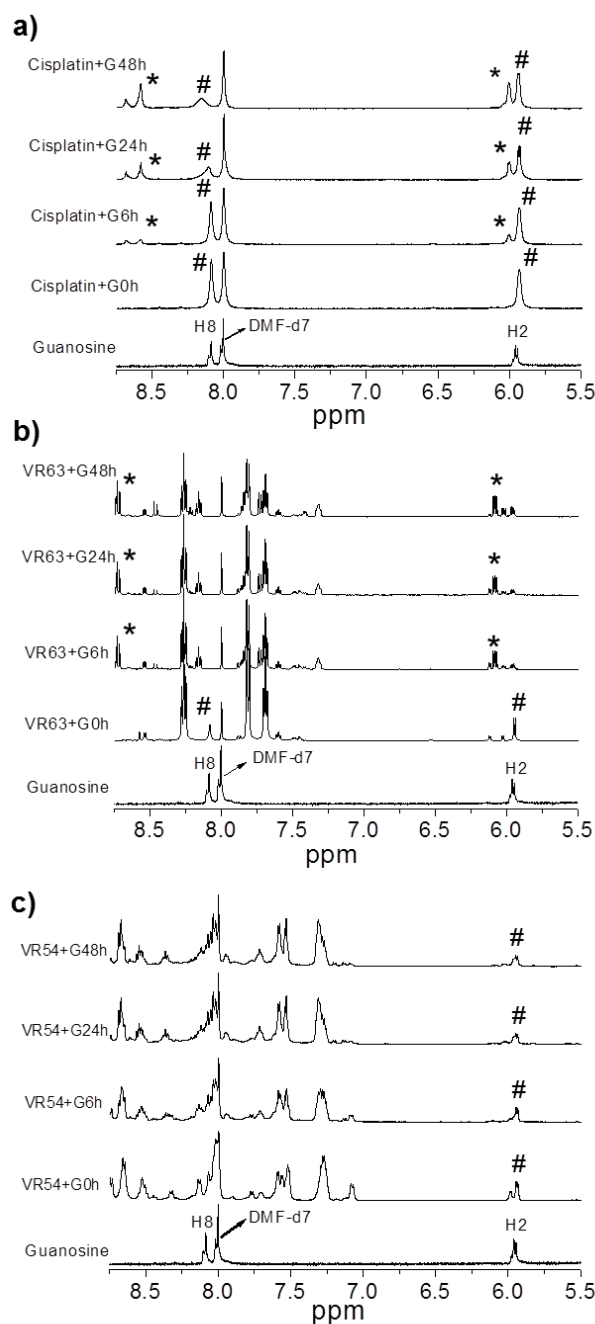


Figure 2. ¹H NMR spectra showing the reaction of a) guanosine (G) with cisplatin, VR63 (b) or VR54 (c) in D₂O over 48 h. Region including H8 and H2 guanosine protons shown. Based on reference [30b], peaks labelled * are Pt-bound guanosine and peaks labelled # are free guanosine. The residual DMF solvent peak used for complex dissolution before addition to guanosine is indicated.

Impact on cancer cell proliferation

As discussed, both drug-resistance, in addition to the absence of identified specific targets in particular cancers, represents a significant on-going challenge for chemotherapy. Therefore, the

effect of VR54 on the proliferation of cisplatin-resistant, A2780CIS ovarian cancer cells was investigated. Quantitative analysis of cell numbers over time in the presence of VR54 indicated a dose-dependent decrease in proliferation with a half inhibitory concentration (IC_{50} , defined as the concentration resulting in 50% reduction in the *fold extent* of proliferation) of $\sim 40 \mu\text{M}$ after 48 h exposure (Figure 3a). Interestingly, negligible signs of cell stress or death were observed, even at higher concentrations of VR54 (Figure 3b). Importantly, although cell proliferation was significantly affected by VR54, the viability of cells (proportion of cells that exclude Trypan-blue) exposed to active doses (40–100 μM) remained unchanged (Figure 3b, and see below, Figure 6); cells numbers reached a plateau after $\sim 48\text{h}$, behaviour which implies cytostatic activity. In contrast, cell numbers in samples treated with cisplatin progressively decreased until cells numbers were negligible; as expected for cytotoxic activity (Figure 3a – see cisplatin data).

To provide an indication of the anti-proliferative capability of VR54 towards a cisplatin-sensitive line compared to resistant cells, a direct comparison between parental (cisplatin-sensitive) A2780 and derivative (cisplatin-resistant) A2780CIS cells was undertaken using a complementary approach. Cells were exposed to a range of concentrations of VR54 or cisplatin for 48 h and the resultant metabolic activity of each cell population was assessed using MTT (3-(4,5-dimethylthiazol-2-yl)-2,5-diphenyltetrazolium bromide) assays (Figure 3c,d).^[31] The mononuclear Ru^{II} parent complex VR52 and mononuclear Pt^{II} complex VR63 were included in parallel to provide information on the structural properties required for the potency of VR54 (Figure S12). As shown in Figure 3c and Table 2, these experiments confirm the impact of VR54 on cell proliferation, and are consistent with the IC_{50} value for VR54 determined by analysis of cell numbers in A2780CIS cells after 48h exposure as determined above.

As expected,^[32] a ten-fold decrease in potency was observed in A2780CIS cells treated with cisplatin compared with the parental line (Figure 3d and Table 2). Significantly, and in direct contrast to results obtained with cisplatin, no cross-resistance to VR54 was observed (Figure 3c), with potency of VR54 almost identical in both cisplatin-sensitive and cisplatin-resistant ovarian cancer cell lines (IC_{50} of 29 and 38 μM for A2780 and A2780CIS cells respectively). The mononuclear Ru^{II} analogue VR52 had negligible effects on either cell line, while the mononuclear Pt^{II} complex VR63 exhibited a four-fold lower potency towards A2780 cells ($IC_{50} = 114 \mu\text{M}$) and had no impact upon A2780CIS cell numbers/viability in the concentration range tested (Table 2 and Figure S12). These results indicate that both the Ru^{II} structural moiety and Pt^{II} metal centre are required for the anti-proliferative behaviour demonstrated by VR54.

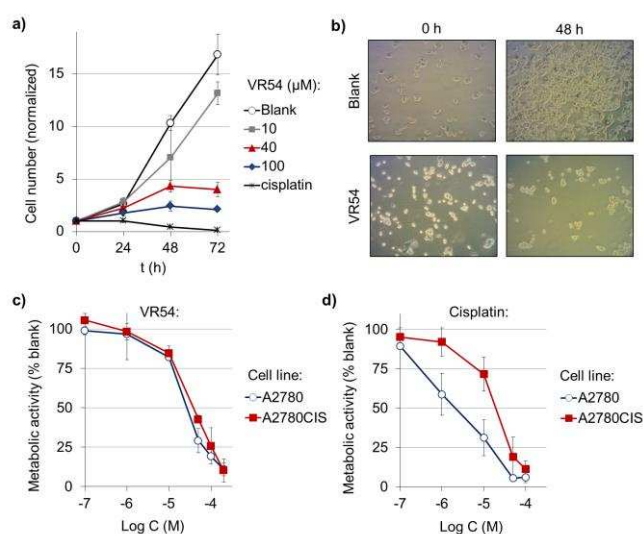


Figure 3. a) Effect of VR54 on A2780CIS cell numbers over time ($n = 3, \pm \text{SD}$). 0.1% DMSO blank and cytotoxic dose of cisplatin (80 μM) included for comparative purposes. Viable cells counted by Trypan-blue exclusion shown. See text for details on the IC_{50} values. b) Images of A2780CIS cells treated with 100 μM VR54. c,d) Effect of VR54 or cisplatin on total metabolic activity of A2780 and A2780CIS cell populations after 48 h exposure ($n = 3, \pm \text{SD}$). See Table 2 for details on the IC_{50} values.

Table 2. Anti-proliferative capability (IC_{50} , (μM) defined as the concentration resulting in 50% reduction in the metabolic activity of the total cell population remaining after the indicated incubation period) of VR52, VR54, VR63 and cisplatin towards A2780 and A2780CIS human ovarian cancer cells.^[a]

Complex	A2780	A2780CIS
VR52	>200	>200
VR54	29 \pm 6	38 \pm 1
VR63	114 \pm 4	>200
Cisplatin	3 \pm 1	30 \pm 1

[a] Determined by MTT assay (48 h incubation time). Data average of three independent experiments $\pm \text{SD}$. See note [31].

Cellular uptake properties

It is well established that the internalization characteristics of metal anticancer complexes may contribute to their efficacy.^[1, 3-4] Given that VR54 has a significantly greater impact on cell proliferation compared to either mononuclear complexes VR52 or VR63, we therefore investigated whether the extent of cellular uptake could explain the difference in bioactivity of each complex.

The relative cellular accumulation of all three compounds in A2780CIS cells was determined using inductively-coupled plasma mass spectrometry (ICP-MS). For cells incubated with solutions of VR52, VR54, VR63 or cisplatin prior to analysis, the

levels of Ru and/or Pt above an untreated control therefore correspond to the cellular accumulation of the relevant complex. As VR54 is a Ru^{II}-Pt^{II} bimetallic system, this approach has the additional advantage as the Ru and Pt concentrations can be obtained separately and directly compared. Results are expressed as the concentration of metal per cell (fmoles/cell). Treatment of A2780CIS cells with VR54 or cisplatin for 24 h resulted in a comparable intracellular Pt content (1.46 ± 0.90 and 1.28 ± 0.13 fmoles Pt/cell for VR54 and cisplatin respectively), indicating VR54 is internalized to similar levels as the established anticancer drug (Figure 4). The Pt content obtained for cells treated with cisplatin is in agreement with literature values.^[33] Assuming an average A2780CIS cell volume of ~ 2 pL,^[34] the Ru and Pt contents (2.06 ± 0.10 and 1.46 ± 0.90 fmol/cell respectively) obtained by this method therefore correspond to an approximate intracellular concentration of 1013 ± 51 and 730 ± 45 μM for Ru and Pt ions respectively in cells treated with VR54 (after blank subtraction). Encouragingly, these values are consistent with each other and indicate the intracellular concentration of VR54 (~ 1 mM) is approximately twenty-fold higher than the external exposure concentration (50 μM). The slight decrease in the absolute levels of Pt content compared to Ru for cells treated with VR54 may reflect the relative sensitivity of the technique towards each metal ion at these relatively low concentrations, however, ICP-MS characterization of isolated VR54 solutions show the expected 1:1 molar ratio of each metal present (Figure S13). Therefore, we cannot exclude the possibility of complex fragmentation upon cellular internalisation, and that VR54 might function as a pro-drug. These results also clearly indicate a greater cellular accumulation of the binuclear conjugate complex VR54 than either mononuclear complexes VR52 or VR63, where data indicate five-fold lower levels of Ru metal ion content for cells incubated with VR52 (VR52 = 0.37 ± 0.03 fmoles Ru/cell) and a 2.5-fold lower Pt content for VR63 (0.58 ± 0.10 fmoles Pt/cell) compared to the results for VR54 (Figure 4). Subsequently normalising these ICP-MS data to cellular protein content (Figure S14), it is clear that VR54, and even the poorly-active VR52, both demonstrate a greater degree of internalisation than certain cytotoxic Ru^{II} polypyridyl DNA intercalators.^[35]

The relationship between an increase in hydrophobicity and extent of cellular uptake of metal complexes has been demonstrated for a range of metal compounds.^[36] In agreement with this concept, the relative cellular uptake levels of VR54, VR52 and VR63, and their anticancer potency, correlate with the hydrophobicity of each complex, as quantified by octanol/water partition coefficient, log P (Figure 4). Despite this clear trend, it is apparent that VR63, which has a comparable log P to cisplatin, has a lower level of cellular uptake - and corresponding decrease in potency - than would be predicted if hydrophobicity were the sole factor in governing internalisation.

To examine the sub-cellular localisation of VR54, A2780 cells were incubated with the complex and cell fractions from the resultant lysates were prepared. The Ru and Pt content in all fractions (nuclear-, mitochondrial- and cytosolic-enriched fractions) were then analysed by ICP-MS. These data show a high proportion of both Pt and Ru content in the nuclear fraction

(Figure S15a). However, upon normalization to protein content of each fraction, it is clear that accumulation of both metals is relatively consistent across these intracellular compartments with a small degree of enrichment (amount of metal/protein per subcellular fraction divided by amount of metal/protein in total cell lysate – see reference^[37]) in the mitochondrial and (for Ru) nuclear fractions (Figure S15b). The differences in the proportions of Ru and Pt in each subcellular fraction again indicates that we cannot exclude the possibility of intracellular fragmentation, and some degree of differential accumulation within distinct cell compartments.

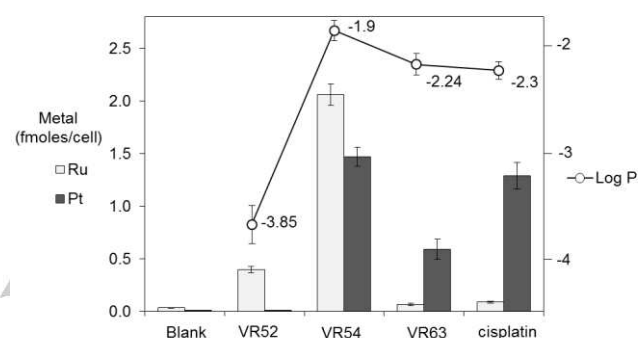


Figure 4. Left hand y-axis: Cellular uptake levels of VR52, VR54, VR63 and cisplatin in A2780CIS cells (50 μM , 24 h), as quantified by ICP-MS analysis of Ru and Pt content ($n = 3$, \pm SD). 0.1% DMSO blank sample included for reference. Right hand y-axis: Log P octanol/water partition coefficients as determined by HPLC (O).

VR54 does not induce apoptosis or necrosis

The intra-strand and inter-strand crosslinks arising from exposure to cisplatin and derivatives activate several DNA damage signalling pathways that ultimately culminate in apoptosis.^[1, 3-4] Therefore, as a starting point to elucidate the cellular mechanism of action of VR54, relative levels of apoptosis after exposure to active doses of the Ru^{II}-Pt^{II} complex were characterised. Firstly, cells were incubated with either VR54 or cisplatin at their respective IC₅₀ concentrations for up to 48 h and the extent of pyknosis and/or karyorrhexis, typical indicators of late-stage apoptosis, was determined. In addition, lysates derived from treated cells were immunoblotted for the active (cleaved) form of the apoptotic marker, caspase-3. Figure 5a shows that, as expected on cisplatin treatment, the fraction of cells with observable nuclear fragmentation increased with time and accounted for over 35 % of cells remaining after 48 h. In contrast, cells incubated with VR54 showed minimal (< 1 %) evidence of chromatin abnormality. Consistent with this, cells treated with the IC₅₀ concentration of cisplatin contained significant levels of activated caspase-3 after 24 h, which continued to increase with time of exposure; clearly indicating an apoptotic response (Figure 5b). In contrast to cisplatin treatment, no activation of caspase-3 was observed in cells treated with an equipotent dose of VR54 (Figure 5b). These results indicate that

exposure to anti-proliferative doses of VR54 does not result in significant levels of apoptosis in A2780CIS cells.

In the absence of an apoptotic response to VR54, we next characterised the levels of total cell death, independent of pathway. To achieve this, A2780CIS cells were treated with anti-proliferative doses of VR54 and the number of Trypan blue-positive (membrane-compromised) cells quantified. While not able to discriminate between cell death pathways, this assay will quantify levels of secondary necrosis, i.e. cells which have lost plasma membrane integrity. Once more, cisplatin was used in parallel as a cytotoxic control. Trypan-blue staining revealed exposure of A2780CIS cells to VR54 did *not* result in the generation of significant levels of membrane-compromised necrotic cells above an untreated control: treatment with the IC₅₀ concentration (determined as described in Table 2) of 40 μ M VR54 resulted in 4 % necrosis and even at doses of 100 μ M VR54 less than 6 % of the cell population has undergone secondary necrosis (Figure 6). Each of these values is comparable to background levels of 3 % Trypan-blue positive cells obtained for untreated control cells. In contrast, exposure to cisplatin generates a large proportion of membrane-compromised cells, where 18 % secondary necrosis is observed for cells treated with the IC₅₀ concentration and the levels of non-viable cells approach 40 % for cells treated with 100 μ M cisplatin; clearly indicating high levels of cell death due to treatment with the cytotoxic compound.

These data provide compelling evidence that VR54 inhibits the proliferation of cancer cells *without* inducing significant levels of cell death. Thus, we conclude VR54 is predominantly acting in a cytostatic, rather than cytotoxic, capacity.^[12]

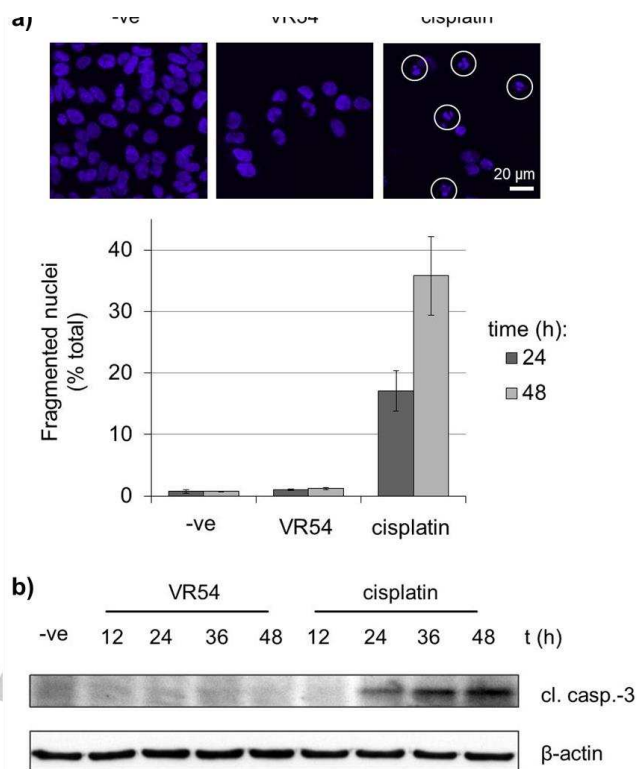


Figure 5. a) Morphological analysis for apoptosis (fragmented nuclei – top, circled) within A2780CIS cell populations incubated with VR54 or cisplatin ($n = 2$, \pm SD). b) Immunoblotting analysis of lysates derived from A2780CIS cells treated either with VR54 or cisplatin for the presence of cleaved caspase-3 (17 kDa fragment), with β -actin as loading control. IC₅₀ concentrations of VR54 and cisplatin used.

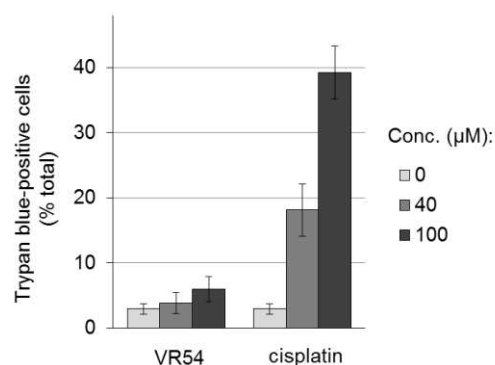


Figure 6. Quantification of levels of secondary necrosis (Trypan Blue-positive, i.e. perforated plasma membrane) A2780CIS cells after exposure to VR54 or cisplatin for 48 h ($n = 3$, \pm SD).

VR54 induces G1 cell cycle arrest

As VR54 exerts an anti-proliferative effect by inducing cytostasis, we hypothesised that cell cycle arrest could explain the inhibition

of cell growth by the complex. To explore the effect of VR54 on the cell cycle, cells were either untreated or exposed to VR54 for 24 h before fixation and flow cytometric analyses. The percentage of cells within each phase of the cell cycle was determined by propidium iodide (PI) staining and DNA content quantification. Figure 7 shows that treatment of cycling A2780CIS cells with 40 μ M VR54 results in a significant concentration-dependent increase in cells in G1 phase compared to the control (65.3 % of the total population in G1 versus 42.7 % respectively), a dramatic apparent reduction in the proportion of S-phase cells (25.5 % versus 42.1 %), and concomitant decrease in the proportion of cells in G2/M phase (9.2 % versus 15.2 %). The higher dose of VR54 (100 μ M) results in an approximately two-fold increase in G1 phase cells (78.9 %) compared to the untreated control (Figure 7). Consistent with the low levels of apoptotic markers described in Figure 5 above, there was no sub-G1 (apoptotic) population in cells treated with VR54.

The large increase in G1 phase cells upon VR54 treatment indicates VR54 inhibits cell proliferation through impeding cell cycle progress, either by inducing cell cycle arrest during G1 phase or by inhibiting the transition from G1 to S phase.

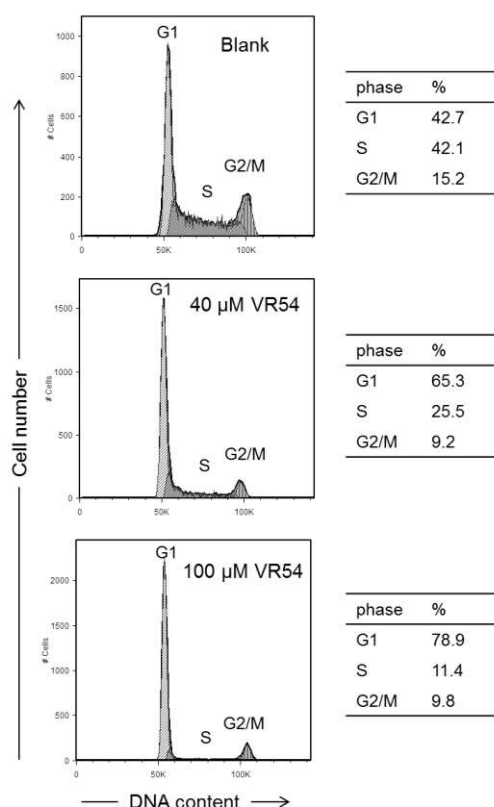


Figure 7. Cell cycle distribution for A2780CIS cells incubated with 0 (blank), 40 μ M or 100 μ M VR54 for 24 h, and subsequently analysed by flow cytometry. DNA content was quantified using propidium iodide (PI).

VR54 does not activate the DNA damage response network

We next set out to elucidate the molecular mechanism responsible for VR54-induced cell cycle arrest. Since cell cycle checkpoints modulate DNA damage/genome integrity responses by controlling the timing of cell cycle progression, and univariate cytometric analyses cannot easily distinguish between cells arrested in G1 or in early S phase, we examined whether VR54-induced cell cycle arrest occurs via activation of DNA damage signalling pathways. Therefore the status of both ATR/Chk1 and ATM/Chk2 checkpoint signalling pathways, which are activated primarily in response to replication stress and double-strand breaks respectively,^[38] was examined. Pathway activation was assessed by determining the extent of phosphorylation of both Chk1 and Chk2 using phospho-specific and total protein antibodies that recognize activated, and all forms of each protein, respectively. Furthermore, the levels of the phosphorylated form of the checkpoint regulator, p53, and a proxy marker of DNA double-strand breaks, phospho-histone H2AX (γ -H2AX), were also determined. As Figure 8 shows, there was no increase in phospho-Chk1 (Ser345) levels in cells treated with VR54 compared to an untreated (-ve) control. In stark contrast, cells incubated with cisplatin exhibited a progressive, time-dependent increase in Chk1 activation, presumably due to replication stress caused by the presence of cisplatin-induced lesions. Similarly, cisplatin, but not VR54, induced significant time-dependent activation of Chk2 (phospho-Chk2, Ser516), as well as an increase in phospho-H2AX (Ser139) and phospho-p53 (Ser10). Again this observation is consistent with the expected generation of cisplatin mediated inter-strand crosslinking, resulting in double-strand breaks and a consequent cellular DNA damage response.

These data indicate that treatment of A2780CIS cells with VR54 does not activate the DNA damage response signalling network, providing confirmation that the cytostatic VR54 operates via a cellular mechanism of action distinct from that of cisplatin.

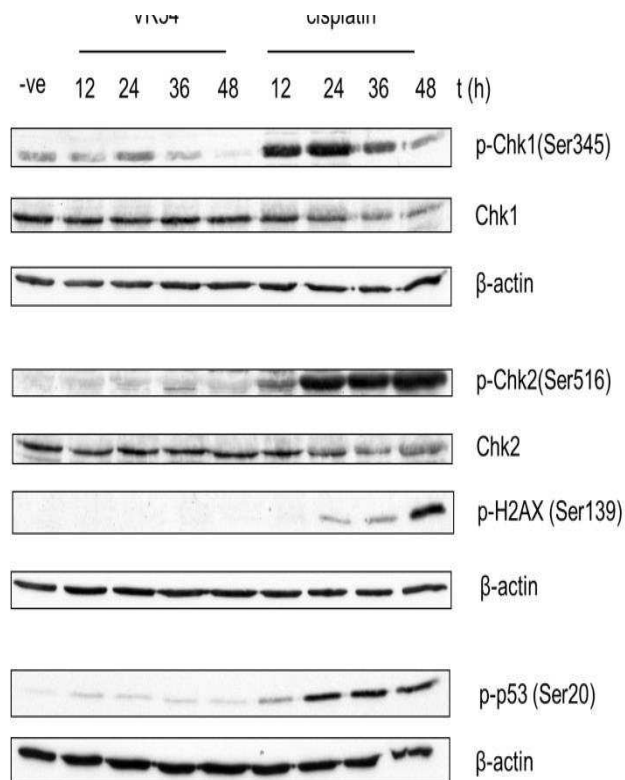


Figure 8. Complex VR54 does not activate DNA damage checkpoints. A2780CIS cells were treated with either 40 μ M VR54 or 30 μ M cisplatin for the indicated times prior to lysate preparation and immunoblotting for anti-phospho Chk1 (Ser345), anti-total Chk1, anti-phospho Chk2 (Ser516), anti-total Chk2, anti-phospho H2AX (Ser139) and anti-phospho p53 (Ser20). β -actin levels were monitored as loading controls.

VR54 up-regulates p27 and inhibits Rb phosphorylation

The transition from G1 to S phase is mediated by activation of cyclin D-Cdk4/6 and cyclin E-Cdk2 protein kinases.^[39] Cdks may be inhibited by specific cyclin-dependent kinase inhibitors (CKIs) such as p21^{CIP1} and p27^{KIP1}, and increased levels of either can result in failure to progress from G1 into S-phase. The former is frequently up-regulated in a p53-dependent manner as part of the DNA damage response.^[40] External signals predominantly modulate p27^{KIP1} levels, with serum deprivation and contact inhibition resulting in its up-regulation, and serum addition or growth factors inducing its down-regulation.^[41] As indicated above, exposure to VR54 results in significant G1/S cell cycle arrest. In the absence of evidence of p53 activation (Figure 8, lower panels), we investigated whether VR54 acts through the up-regulation of the G1 Cdk inhibitor, p27^{KIP1} by determining levels of p27^{KIP1} expression as a result of treatment with VR54. Serum starvation was used as a positive control for up-regulation of p27^{KIP1}.^[41]

Western blot analysis of A2780CIS cells treated with VR54 for 24 h showed a significant dose-dependent increase in the levels of p27^{KIP1} compared to an untreated control (Figure 9a, upper and lower panels). Quantifying this increase, treatment of

cells with 40 μ M VR54 resulted in a ~ 2-fold increase in p27^{KIP1} levels, while cells exposed to 100 μ M VR54 resulted in levels of p27^{KIP1} significantly greater than observed in serum-starved (i.e. quiescent) cells, a four-fold increase compared to the (serum-containing) untreated control (Figure 9a, lower panels). p27 levels in cells treated with 100 μ M VR52 or VR63 showed comparable p27^{KIP1} levels to the untreated control, consistent with the absence of an effect of either mononuclear complex on cell proliferation at these concentrations. The increased p27^{KIP1} levels arising from exposure to VR54 directly correlate with the inhibition of cell growth and cell cycle accumulation in G1 phase.

In order to confirm that VR54 exerts its cell cycle inhibitory effect via up-regulation of p27^{KIP1} and consequent inhibition of cyclin-Cdk complexes, we examined the effect of VR54 on the activation status of the tumour suppressor retinoblastoma protein (Rb), which plays a key role in the exit from G1 phase.^[13] During the progression from G1 into S phase, active hypophosphorylated Rb is deactivated via phosphorylation by the cyclin D-Cdk4/6 and cyclin E-Cdk2 kinases to facilitate cell cycle progression.^[42] Using antibodies that recognize either phosphorylated Rb (at Ser780) or total Rb levels, we examined the phosphorylation status of Rb in VR54-treated cells by western blot analysis to determine the activation status of this pathway. Figure 9b (upper panel) shows cells exposed to VR54 exhibit a progressive, concentration-dependent decrease in levels of p-Rb phosphorylated at Ser 780, indicating the strong inhibition of Rb phosphorylation at this site. Consistent with this observation, the ratio of hyper-phosphorylated Rb to hypophosphorylated Rb decreased with exposure to VR54 (Figure 9b, middle panel). These results indicate the phosphorylation of Rb is dramatically inhibited by VR54 and are in agreement with the concept that VR54 up-regulates p27^{KIP1}. In order to investigate any contribution of p21 to the hypophosphorylation of Rb, we undertook western blot analysis of p21 levels following exposure to VR54, however, no increase in p21 was observed after 24 h exposure (Figure S16).

We therefore conclude that the mechanism of action of VR54 is through the up-regulation of p27^{KIP1} and resultant inhibition of Rb phosphorylation. The inhibition of Rb phosphorylation acts to block cell cycle entry into S phase at the G1 restriction point, culminating in G1 cell cycle arrest and the inhibition of cell growth (Scheme 3).

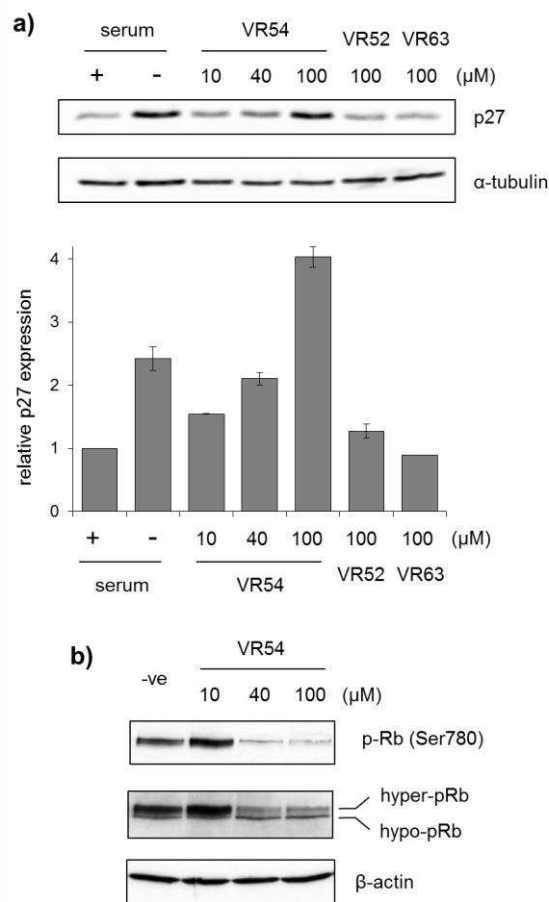
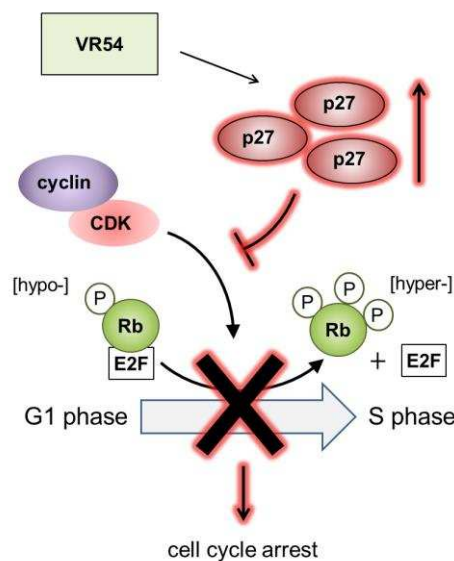


Figure 9. Exposure to VR54 results in p27^{KIP1} up-regulation and inhibition of Rb phosphorylation. a) A2780CIS cells growing in serum-containing medium were treated with 0.1% DMSO (control), VR54, VR52 or VR63 at the stated concentrations for 24 h prior to lysate preparation and immunoblotting with anti-p27 antibodies. Serum-starved cells (24 h) were employed as a positive control. α -tubulin levels were monitored as a loading control. Data average of two technical repeats. b) A2780CIS cells were incubated with VR54 or a negative control (0.1% DMSO) for 24 h prior to lysate preparation and immunoblotting with anti-phospho-Rb (Ser780) and anti-total Rb antibodies, independent of phosphorylation state, where hypo-phosphorylated Rb (hypo-pRb) is the active form and hyper-phosphorylated Rb (hyper-pRb) is the inactive form. β -actin levels were used as a loading control. All results are representative of two independent experiments.



Scheme 3. Diagram illustrating the proposed mechanism of action of VR54.

Discussion

While numerous anticancer metal complexes suitable for conventional cytotoxic chemotherapy have been described, metal compounds that inhibit cancer cell proliferation by alternative modes of action have been neglected. In particular, the role of cytostatic metal complexes that interfere with cancer cell cycle regulatory pathways to halt cell growth is an unexplored area of study.

In this study, we prepared the Ru^{II}-Pt^{II} binuclear complex VR54, which links a Pt^{II}(Cl)(DMSO) moiety to a Ru^{II}-terpyridine group through the ditopic terpyridyl ligand tppyma, and the mononuclear Ru^{II}(tppyma) complex VR52 (Scheme 1). Both VR52 and VR54 display reasonable reversible binding affinities for DNA, where they interact *via* a non-intercalative mode of binding, most likely groove-binding accompanied by an electrostatic contribution (Figure 1). Somewhat unexpectedly, VR54 does not bind covalently to guanosine, unlike cisplatin (Figure 2c). It is known that DMSO substitution in solution decreases the activity of cisplatin,^[43] while a similar lack of reactivity towards nucleotide coordination has been observed for several Pt^{II}(Cl)(DMSO) complexes.^[44] However, DMSO substitution alone cannot explain the lack of reactivity of VR54, as significant reactivity was observed with VR63 (Figure 2b). Thus, the lack of reactivity of VR54 towards guanosine is likely due to a combination of DMSO substitution and the electron-withdrawing properties of the attached Ru^{II}-tppyma complex.

Our cellular studies nonetheless show VR54 inhibits the proliferation of A2780 ovarian cancer cells and, importantly, the potency of its anti-proliferative effect observed is retained in cisplatin-resistant A2780CIS cells (Figure 3). In either case, the potency of VR54 is not substantially different from that of tamoxifen,^[18] used in the treatment of estrogen receptor+ breast tumours. These data suggest that there is potential for future

design and optimisation of metal complexes that are potently anti-proliferative, but are not subject to the some of the mechanisms which give rise to platinum resistance.

Considering that the mononuclear Ru^{II} complex VR52 displays no observable bio-activity under the same conditions, while the mononuclear Pt^{II} compound VR63 demonstrates significantly weaker effects, this implies that both Ru^{II} and Pt^{II} components contribute to the behaviour demonstrated by VR54 (Table 2). While, as discussed below, the platinum centre of VR54 does not react in the traditionally expected way, our quantitative cellular measurements indicate a five-fold higher intracellular concentration of VR54 compared to the mononuclear Ru^{II} complex VR52 (Figure 4). We postulate the addition of the Pt^{II}(Cl)(DMSO)⁺ monocationic group promotes cellular accumulation. Such an effect could either operate through a relative increase in hydrophobicity of the Ru^{II}-Pt^{II} complex promoting passive diffusion across the cell membrane,^[45] or alternatively by targeting a specific transporter protein through a recognition motif,^[46] as the correlation of cellular accumulation with log P does not necessarily infer passive transport as the dominant uptake mechanism for transition metal compounds.^[47]

Several strong lines of evidence indicate that VR54 inhibits cancer cell growth via a cytostatic mechanism, and not via a cytotoxic mechanism involving the platination of nucleobases, and consequent accumulation of toxic double-strand breaks. Firstly, VR54 demonstrates a concentration dependent reduction in the rate of proliferation, but crucially in the absence of any reduction in seeded cell numbers (Figure 3a) or the appearance of any of the markers of apoptotic or other cell death (Figures 5 and 6). Secondly, it is well established that platinum-based drugs with labile coordination sites induce a DNA damage response involving the activation of both ATR/Chk1 and ATM/Chk2 signalling pathways following the formation of bulky inter- and intra-strand cross-links, via platination of the N₇ of guanine bases.^[4] Both ATM and ATR protein kinases contribute to the phosphorylation and stabilization of p53 which ultimately results in late G1/early S phase arrest and apoptosis.^[48] However, no reaction was observed between VR54 and guanosine in cell-free studies, even after prolonged incubation (Figure 2), while, in cellular studies, VR54 did not induce histone H2AX phosphorylation, a direct marker of DNA double-strand breaks, nor did the complex have any effect on the phosphorylation state of either Chk1 or Chk2 checkpoint kinases, indicating no component of the DNA damage response pathway to be activated (Figure 8).

Thirdly, we found the mechanism by which VR54 inhibits proliferation of A2780CIS cells to be through a strong G1 cell cycle arrest resulting from the induction of elevated levels of the CKI, p27^{KIP1} and the consequent inhibition of Rb phosphorylation (Figures 7 and 9). The transition from G1 into S phase, known as the restriction point, is mediated by activation of the S phase transcription factor, E2F, which binds to, and is inhibited by, hypo-phosphorylated (active) Rb. In the presence of growth factors, cyclin D-Cdk4/6 and cyclin E-Cdk2 protein kinases bring about Rb inactivation (hyper-phosphorylated Rb) which in turn releases transcriptionally active E2F, thereby ensuring the G1-S

transition (Scheme 3).^[13] Thus p27^{KIP1} is a tumour suppressor that plays a critical role in the key regulatory system controlling cell proliferation.^[19] By interfering with cyclin-Cdk mediated phosphorylation of Rb bound to E2F, p27^{KIP1} prevents E2F release and therefore entry into S phase. It may be noted that the cytostatic effect of VR54 becomes apparent after ~48 h (Figure 3a). This reflects the asynchronous nature of the cell population with respect to the cell cycle. As the intracellular concentration of VR54 builds up with resultant increases in p27^{KIP1}, those cells which have passed the restriction point (late G1) are committed to undergo a round of cell division (thus increasing cell numbers), and it is only as time progresses that cells moving through the cell cycle encounter the restriction point block at the G1/S transition, resulting in overall cytostasis. Importantly, neither VR52 nor VR63 have any effect on p27^{KIP1} levels, reinforcing the notion that both Ru^{II} and Pt^{II} components contribute to the cellular behaviour demonstrated by VR54.

Up-regulation of p27^{KIP1} can be indirectly induced as a consequence of the introduction of DNA damage lesions through a p21-dependent mechanism.^[49] However, since treatment with VR54 neither increases p21 levels (Figure S16), nor activates p53 (Figure 8), a pre-requisite for the up-regulation of p21^{CIP1},^[50] in response to DNA damage, we conclude VR54 cannot be up-regulating p27^{KIP1} either through a mechanism involving p53-mediated genomic stress induced cell-cycle arrest, or other p53 independent p21-mediated mechanisms. Furthermore, as the DNA damage response network is known to contribute in part to cisplatin-resistance,^[51] it seems likely that the radically different mechanism of action of VR54 compared to cisplatin is responsible for the lack of cross-resistance towards a cisplatin-resistant cell line.

The cellular mechanism of VR54 has wider significance. Unsurprisingly, expression of restriction point mediators, including Rb, cyclin D, as well as p27^{KIP1} itself, are frequently altered in a wide range of cancers,^[13] as distortion of this regulatory system uncouples cell cycle progression from autocrine and paracrine signaling-mediated growth factor control, a key aspect of neoplastic progression.^[41] As a result, the evaluation of p27^{KIP1} levels are utilized to predict response to both chemotherapy and radiotherapy treatments, as well as endocrine manipulation,^[52] leading to calls for the development of new therapeutics capable of p27^{KIP1} up-regulation.^[41]

If personalized cancer therapy is to be realized, future targeted treatments, either as first line treatment or to overcome resistance, will require considerable understanding of individual cancer cell survival pathways. In this context, VR54 and derivatives may have considerable potential in association with targeted therapeutic regimes aimed at inhibiting progression through G1. For example, the effectiveness of the cytostatic drug, trastuzumab (Herceptin) in inducing cell cycle arrest in G1 phase and suppressing growth of human breast cancer depends, not only on the over-expression of the receptor tyrosine kinase HER2 in tumours, but also the presence of the cyclin-dependent kinase inhibitor protein, p27^{KIP1}, to prevent the G1/S transition.^[14a, 53] Similarly, tamoxifen resistance in breast cancer has been shown to involve reduced levels of p27^{KIP1}, *via* up-

regulation of miRNAs-221/222, while genetic over-expression of p27^{KIP1} has been shown to restore tamoxifen resistance.^[54]

It follows that a combination of targeted regimens with selective chemotherapeutics may well represent an important developmental step in stratified approaches to cancer therapy.^[55] Considering these points, the therapeutic application of VR54 and derivatives may involve combinatorial strategies alongside conventional targeted regimens. In such regimes, the low cytotoxicity of VR54 would be predicted to be an advantageous property.

The molecular mechanism by which VR54 up-regulates p27^{KIP1} is of great interest. Cellular levels of p27^{KIP1} are controlled by a highly complex multi-component network of signalling, transcriptional, translational and protein degradation pathways.^[50] One intriguing possibility is that complex VR54 up-regulates p27^{KIP1} via subtle alteration of the cellular epigenome, either by affecting p27^{KIP1} transcription directly or by altering the levels or functionality of one or more of its upstream regulators.^[56] Work involving genome-wide expression profiling in the presence and absence of VR54 may be revealing in this regard.

Conclusions

In summary, we report the synthesis and characterisation of a cytostatic binuclear ruthenium(II)-platinum(II) bis(terpyridyl) complex, VR54, which inhibits the proliferation of ovarian cancer cells through the up-regulation of the cyclin-dependent kinase inhibitor p27^{KIP1}, resulting in the inhibition of Rb phosphorylation and G1 cell cycle arrest. At both the molecular and cellular level, VR54 functions by a radically different mechanism to cisplatin, showing that it belongs to an entirely different category to any other platinum-based therapeutic candidate, and expands the potential scope of activity for metal-based anticancer complexes for inclusion within targeted therapy regimes.

Experimental Section

Synthesis of [Ru(tpy)(tpypma)](PF₆)₂ (VR52). [(tpy)Ru(tpy-a)](PF₆)₂^[21] (200 mg, 0.21 mmol) was dissolved in the minimum amount of dry CH₃CN (1 mL) and 30 mL of dry MeOH. 2-Pyridinecarboxaldehyde (0.040 mL, 0.422 mmol) was added and the reaction mixture was refluxed for 9 h with continuous stirring. After cooling to room temperature, the solvent was evaporated under reduced pressure. The reaction mixture was re-dissolved in 100 mL of dry MeOH and refluxed for 1 h followed by the addition of excess of NaBH₄ (100 mg). The reaction mixture was allowed to reflux for 3 h with continuous stirring. The reaction mixture was cooled to room temperature and 10 mL of distilled water was added to remove excess NaBH₄. Saturated KPF₆ (2 mL) solution was added to exchange the counter anions and the metal complex was extracted by the solvent extraction method using CH₂Cl₂/H₂O. A minimum amount of CH₃CN (0.5 mL) was added in order to bring the complex in to the organic layer from aqueous layer. This crude compound was purified by column chromatography, using silica gel as the stationary phase and CH₃CN as the mobile phase. Yield: 54.7 % (120 mg, 0.115 mmol). ¹H NMR (500 MHz, DMF-d₇) δ 9.54 (s, 2H), 9.34 – 9.31 (m, 4H), 9.06 (d, *J* = 8.0 Hz, 2H), 8.67 (d, *J* = 4.6 Hz, 1H), 8.61 (d, *J* =

8.1 Hz, 1H), 8.43 (d, *J* = 8.7 Hz, 2H), 8.14 – 8.11 (m, 5H), 7.91 (d, *J* = 5.2 Hz, 2H), 7.72 (d, *J* = 5.4 Hz, 2H), 7.58 (d, *J* = 7.8 Hz, 1H), 7.40 – 7.35 (m, 6H), 7.07 (d, *J* = 8.7 Hz, 2H), 4.69 (s, 2H). Elemental analysis (as (PF₆)₂ salt) (C₄₂H₃₂F₁₂N₈P₂Ru). Calcd: C, 48.52; H, 3.10; N, 10.78; Found: C, 48.43; H, 3.13; N, 10.59. ESIMS (*m/z*): 895.7, [M-PF₆]⁺.

Synthesis of [Ru(tpy)(tpypma)Pt(Cl)(DMSO)](PF₆)₃ (VR54). Step 1 – formation of intermediate complex [Ru(tpy)(tpypma)Pt(Cl)₂](Cl)₂ (VR53). Complex VR52 was converted to its chloride salt by anion metathesis and dried under vacuum. Potassium tetrachloro platinate (32 mg, 0.077 mmol) was dissolved in 10 mL water, followed by the addition of complex VR52 (80 mg, 0.097 mmol). The reaction mixture was stirred at room temperature (25 °C) for 3 h in the dark. The precipitate formed (VR53) was collected by centrifugation and washed with water (3 x 2 mL) to remove excess K₂[PtCl₄] before drying under vacuum. Yield: 64.8 % (54.5 mg, 0.050 mmol). ESIMS *m/z*: [M]²⁺ 507.03. Step 2 – conversion of VR53 to VR54. Complex VR53 (50 mg, 0.046 mmol) was dissolved in DMSO: H₂O (1: 9). The reaction mixture was stirred at room temperature (25 °C) for 120 h in the dark. The addition of saturated KPF₆ solution (1 mL) afforded a deep red coloured precipitate (complex VR54), which was collected by using grade-4 crucible followed by washing with water (3 x 2 mL). Yield: 36.9 % (26 mg, 0.017 mmol). ¹H NMR (500 MHz, DMF-d₇) δ 9.46 (s, 2H), 9.25 – 9.22 (m, 4H), 8.99 (d, *J* = 8.1 Hz, 2H), 8.65 (d, *J* = 5.0 Hz, 1H), 8.61 (s, 1H), 8.36 (d, *J* = 8.7 Hz, 2H), 8.12 (dd, *J* = 7.1, 4.2 Hz, 5H), 7.89 (s, 2H), 7.70 (d, *J* = 5.4 Hz, 2H), 7.55 (d, *J* = 7.8 Hz, 1H), 7.38 – 7.34 (m, 5H), 7.22 (s, 1H), 7.05 (d, *J* = 8.7 Hz, 2H), 4.67 (d, *J* = 3.6 Hz, 2H), 3.35 (s, 6H). ¹⁹⁵Pt NMR (DMSO-d₆), δ (ppm): -2967 (s, 1Pt). Elemental analysis (as Cl₃ salt, C₄₄H₃₈Cl₄N₈OPtRuS). Calcd: C, 45.37; H, 3.29; N, 9.62; Found: C, 45.21; H, 3.30; N, 9.47. ESIMS (*m/z*): [M]³⁺ Calcd 352.7084; Found, 352.7087.

Synthesis of [Pt(amp)(Cl)(DMSO)]⁺ (VR63). [Pt(Cl)₂(amp)]^[22] (100 mg, 0.26 mmol) was dissolved in DMSO: H₂O (1: 9). The reaction mixture was stirred at room temperature for 2h in the dark. The addition of saturated KPF₆ solution (1 mL) afforded a pale yellow coloured precipitate, which was collected by using grade-3 crucible followed by washing with water (3 x 2 mL) and diethyl ether (2 x 5 mL). Yield: 50.7 % (76 mg, 0.135 mmol). ¹H NMR (500 MHz, DMF-d₇) δ 9.06 (dd, *J* = 5.9, 0.8 Hz, 1H), 8.39 (dd, *J* = 7.8, 6.3 Hz, 1H), 7.99 (dd, *J* = 7.9, 0.4 Hz, 1H), 7.84 – 7.81 (m, 1H), 6.86 (s, 2H), 4.74 (t, *J* = 5.9 Hz, 2H), 3.69 (s, 6H).. ¹⁹⁵Pt NMR (DMSO), δ (ppm): -3142 (s, 1Pt). Elemental analysis (as Cl salt, C₆H₁₄ClN₂OPTS). Calcd: C, 21.25; H, 3.12; N, 6.19; Found: C, 21.18; H, 3.1; N, 6.17. ESIMS (*m/z*): [M]⁺ Calcd, 416.016; Found, 416.015.

For full experimental details and protocols see supporting information.

Acknowledgements

This work was supported by Yorkshire Cancer Research (C. S.), and EPSRC/Wellcome Trust Fellowships (M.R.G.). We gratefully acknowledge the financial support of the British Council-Indian DST-UKIERI scheme DBT (India) and CSIR Network Project (M2D-CSC-0129) (V.R., A.D. and J.A.T.). Mass Spectrometry was undertaken in the Sheffield Mass Spectrometry Facility, supported by Yorkshire Cancer Research (SHENDO1). We thank D. Sutton for technical support, M. Hewins for flow cytometry, N. Bramall for ICP-MS and Dr D. Robinson for light microscopy support (Wellcome Trust, 077544).

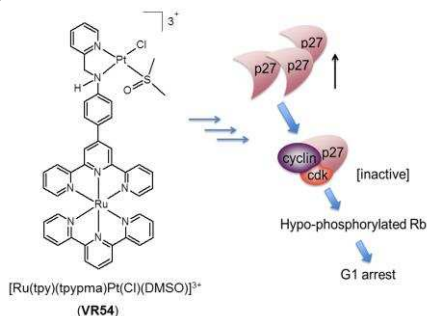
Keywords: antitumor agents • platinum drugs • ruthenium terpyridine • cytostatic • p27KIP1

- [1] L. R. Kelland, *Nat. Rev. Cancer* **2007**, *7*, 573-584.
- [2] P. M. Takahara, A. C. Rosenzweig, C. A. Frederick, S. J. Lippard, *Nature* **1995**, *377*, 649-652.
- [3] Y. Jung, S. J. Lippard, *Chem. Rev.* **2007**, *107*, 1387-1407.
- [4] Z. H. Siddik, *Oncogene* **2003**, *22*, 7265-7279.
- [5] a) S. H. van Rijjt, P. J. Sadler, *Drug Discov. Today* **2009**, *14*, 1089-1097; b) G. Gasser, I. Ott, N. Metzler-Nolte, *J. Med. Chem.* **2011**, *54*, 3-25.
- [6] a) E. Alessio, G. Mestroni, A. Bergamo, G. Sava, *Curr. Top. Med. Chem.* **2004**, *15*, 1525-1535; b) C. Scolaro, A. Bergamo, L. Brescacin, R. Delfino, M. Cocchiello, G. Laurenczy, T. J. Geldbach, G. Sava, P. J. Dyson, *J. Med. Chem.* **2005**, *48*, 4161-4171.
- [7] L. H. Hurley, *Nat. Rev. Cancer* **2002**, *2*, 188-200.
- [8] T. A. Hensing, N. H. Hanna, H. H. Gillenwater, M. G. Camboni, C. Allievi, M. A. Socinski, *Anti-Cancer Drugs* **2006**, *17*, 697-704.
<http://www.cancer.gov/cancertopics/factsheet/Therapy/targeted>
- [9] I. Collins, P. Workman, *Nat. Chem. Biol.* **2006**, *2*, 689-700.
- [11] a) H. Al-Nakhle, P. A. Burns, M. Cummings, A. M. Hanby, T. A. Hughes, S. Satheesha, A. M. Shaaban, L. Smith, V. Speirs, *Cancer Res.* **2010**, *70*, 4778-4784; b) D. Garcia, M. R. Warr, C. P. Martins, L. Brown Swigart, E. Passequé, G. I. Evan, *Genes Dev.* **2011**, *25*, 1746-1757.
- [12] Cytostasis is defined as the inhibition of cell growth and multiplication. See, for example, S. Pervin, R. Singh and G. Chaudhuri, *Proc. Natl. Acad. Sci.*, 2001, *98*, 3583-3588. For a discussion on the relationship between cytostasis and cytotoxicity in anticancer therapeutics, see: O. Rixe, T. Fojo, *Clin. Cancer Res.* 2007, *13*, 7280-7287.
- [13] M. Malumbres, M. Barbacid, *Nat. Rev. Cancer* **2001**, *1*, 222-231.
- [14] a) X.-F. Le, F.-X. Claret, A. Lammayot, L. Tian, D. Deshpande, R. LaPushin, A. M. Tari, R. C. Bast, *J. Biol. Chem.* **2003**, *278*, 23441-23450; b) X. F. Le, I. Bedrosian, W. Mao, M. Murray, Z. Lu, K. Keyomarsi, M. H. Lee, J. Zhao, R. C. Bast, *Cell Cycle* **2006**, *5*, 1654-1661.
- [15] a) I. Chu, K. Blackwell, S. Chen, J. Slingerland, *Cancer Res.* **2005**, *65*, 18-25; b) W. Xia, R. J. Mullin, B. R. Keith, L.-H. Liu, H. Ma, D. W. Rusnak, G. Owens, K. J. Allgood, N. L. Spector, *Oncogene* **2002**, *21*, 6255-6263.
- [16] I. Chu, J. Sun, A. Arnaout, H. Kahn, W. Hanna, S. Narod, P. Sun, C.-K. Tan, L. Hengst, J. Slingerland, *Cell* **2007**, *128*, 281-294.
- [17] a) L. K. Dunnwald, M. A. Rossing, C. I. Li, *Breast Cancer Research* **2007**, *9*, R6; b) G. Early Breast Cancer Trialists' Collaborative, *Lancet*, *378*, 771-784.
- [18] H. Seeger, J. Huober, D. Wallwiener, A. O. Mueck, *Horm. Metab. Res.* **2004**, *36*, 277-280.
- [19] a) H. Toyoshima, T. Hunter, *Cell* **1994**, *78*, 67-74; b) K. Nakayama, N. Ishida, M. Shirane, A. Inomata, T. Inoue, N. Shishido, I. Horii, D. Y. Loh, K.-i. Nakayama, *Cell* **1996**, *85*, 707-720; c) M. L. Fero, M. Rivkin, M. Tasch, P. Porter, C. E. Carow, E. Firpo, K. Polyak, L.-H. Tsai, V. Broudy, R. M. Perimutter, K. Kaushansky, J. M. Roberts, *Cell* **1996**, *85*, 733-744; d) H. Kiyokawa, R. D. Kineman, K. O. Manova-Todorova, V. C. Soares, E. S. Hoffman, M. Ono, D. Khanam, A. C. Hayday, L. A. Frohman, A. Koff, *Cell* **1996**, *85*, 721-732.
- [20] M. Burgess, S. Puhalla, *Front Oncol.* **2014**, *4*, 19.
- [21] a) E. C. Constable, A. M. W. Cargill Thompson, *J. Chem. Soc., Dalton Trans.* **1994**, 1409-1418; b) J. Wang, G. S. Hanan, *Synlett* **2005**, *8*, 1251-1254.
- [22] a) M. L. Niven, G. C. Percy, D. A. Thornton, *J. Mol. Struct.* **1980**, *68*, 73-80; b) H. Brunner, M. Schmidt, H. Schönenberger, *Inorg. Chim. Acta* **1986**, *123*, 201-207.
- [23] J. H. Price, A. N. Williamson, R. F. Schramm, B. B. Wayland, *Inorg. Chem.* **1972**, *11*, 1280-1284.
- [24] U. Bierbach, T. W. Hambley, N. Farrell, *Inorg. Chem.* **1998**, *37*, 708-716.
- [25] E. A. Medlycott, G. S. Hanan, *Coord. Chem. Rev.* **2006**, *250*, 1763-1782.
- [26] a) C. Metcalfe, J. A. Thomas, *Chem. Soc. Rev.* **2003**, *32*, 215-224; b) M. R. Gill, J. A. Thomas, *Chem. Soc. Rev.* **2012**, *41*, 3179-3192.
- [27] a) M. Milkevitch, H. Storré, E. Brauns, K. J. Brewer, B. W. Shirley, *Inorg. Chem.* **1997**, *36*, 4534-4538; b) R. L. Williams, H. N. Toft, B. Winkel, K. J. Brewer, *Inorg. Chem.* **2003**, *42*, 4394-4400; c) A. Jain, J. Wang, E. R. Mashack, B. S. J. Winkel, K. J. Brewer, *Inorg. Chem.* **2009**, *48*, 9077-9084; d) S. L. H. Higgins, A. J. Tucker, B. S. J. Winkel, K. J. Brewer, *Chem. Commun.* **2012**, *48*, 67-69; e) A. Petitjean, J. K. Barton, *J. Am. Chem. Soc.* **2004**, *126*, 14728-14729; f) K. van der Schilden, F. Garcia, H. Kooijman, A. L. Spek, J. G. Haasnoot, J. Reedijk, *Angew. Chem. Int. Ed.* **2004**, *43*, 5668-5670; g) K. Sakai, H. Ozawa, H. Yamada, T. Tsubomura, M. Hara, A. Higuchi, M.-a. Haga, *Dalton Trans.* **2006**, 3300-3305; h) A. Herman, J. M. Tanski, M. F. Tibbetts, C. M. Anderson, *Inorg. Chem.* **2007**, *47*, 274-280; i) C. M. Anderson, I. R. Taylor, M. F. Tibbetts, J. Philpott, Y. Hu, J. M. Tanski, *Inorg. Chem.* **2012**, *51*, 12917-12924.
- [28] J. D. McGhee, P. H. von Hippel, *J. Mol. Biol.* **1974**, *86*, 469-489.
- [29] C. Metcalfe, C. Rajput, J. A. Thomas, *J. Inorg. Biochem.* **2006**, *100*, 1314-1319.
- [30] a) E. Pantoja, A. Gallipoli, S. van Zutphen, S. Komeda, D. Reddy, D. Jaganyi, M. Lutz, D. M. Tooke, A. L. Spek, C. Navarro-Ranninger, J. Reedijk, *J. Inorg. Biochem.* **2006**, *100*, 1955-1964; b) N. J. Wheate, B. J. Evison, A. J. Herlt, D. R. Phillips, J. G. Collins, *Dalton Trans.* **2003**, 3486-3492.
- [31] In addition to cytotoxicity, MTT assays will additionally quantify cytostatic behaviour, or a combination of either anti-proliferative effect, as the metabolic activity measured is proportional to both cell viability and cell number. This is particularly relevant when the drug incubation time is [significantly] greater than the cell line doubling time. See, for example, C. R. Cardoso, M. V. S. Lima, J. Chaleski, E. J. Peterson, T. Venâncio, N. P. Farrell, R. M. Carlos, *J. Med. Chem.* 2014, *57*, 4906-4915.
- [32] Y. Najajreh, J. M. Perez, C. Navarro-Ranninger, D. Gibson, *J. Med. Chem.* **2002**, *45*, 5189-5195.
- [33] D. Screnci, M. J. McKeage, P. Galetti, T. W. Hambley, B. D. Palmer, B. C. Baguley, *Br. J. Cancer* **2000**, *82*, 966-972.
- [34] <http://meetinglibrary.asco.org/content/116865-132>
- [35] U. Schatzschneider, J. Niesel, I. Ott, R. Gust, H. Alborzinia, S. Wölfl, *ChemMedChem* **2008**, *3*, 1104-1109.
- [36] C. A. Puckett, R. J. Ernst, J. K. Barton, *Dalton Trans.* **2010**, *39*, 1159-1170.
- [37] C. de Duve, B. C. Pressman, R. Gianetto, R. Wattiaux, F. Appelmans, *Biochem. J.* **1955**, *60*, 604-617.
- [38] a) C. Hall-Jackson, D. A. E. Cross, N. Morrice, C. Smythe, *Oncogene* **1999**, *18*, 6707-6713; b) E. Bolderson, J. Scorch, T. Helleday, C. Smythe, M. Meuth, *Hum. Mol. Genet.* **2004**, *13*, 2937-2945.
- [39] D. Resnitzky, S. I. Reed, *Mol. Cell. Biol.* **1995**, *15*, 3463-3469.
- [40] W. S. El-Deiry, J. W. Harper, P. M. O'Connor, V. E. Velculescu, C. E. Canman, J. Jackman, J. A. Pietenpol, M. Burrell, D. E. Hill, Y. Wang, K. G. Wiman, W. E. Mercer, M. B. Kastan, K. W. Kohn, S. J. Elledge, K. W. Kinzler, B. Vogelstein, *Cancer Res.* **1994**, *54*, 1169-1174.
- [41] C. J. Sherr, J. M. Roberts, *Genes Dev.* **1999**, *13*, 1501-1512.
- [42] J. W. Harbour, D. C. Dean, *Nat. Cell Biol.* **2000**, *2*, E65-E67.
- [43] a) W. I. Sundquist, K. J. Ahmed, L. S. Hollis, S. J. Lippard, *Inorg. Chem.* **1987**, *26*, 1524-1528; b) M. D. Hall, K. A. Telma, K.-E. Chang, T. D. Lee, J. P. Madigan, J. R. Lloyd, I. S. Goldlust, J. D. Hoeschele, M. M. Gottesman, *Cancer Res.* **2014**, *74*, 3913-3922.
- [44] a) U. Bierbach, J. D. Roberts, N. Farrell, *Inorg. Chem.* **1998**, *37*, 717-723; b) A. Muscella, N. Calabriso, S. A. De Pascali, L. Urso, A. Ciccarese, F. P. Fanizzi, D. Mignoni, S. Marsigliante, *Biochem. Pharmacol.* **2007**, *74*, 28-40.

- [45] a) C. A. Puckett, J. K. Barton, *J. Am. Chem. Soc.* **2007**, *129*, 46-47; b) C. A. Puckett, J. K. Barton, *Biochemistry* **2008**, *47*, 11711-11716.
- [46] P. D. Dobson, D. B. Kell, *Nat. Rev. Drug Discov.* **2008**, *7*, 205-220.
- [47] a) M. R. Gill, J. Garcia-Lara, S. J. Foster, C. Smythe, G. Battaglia, J. A. Thomas, *Nat. Chem.* **2009**, *1*, 662-667; b) M. R. Gill, D. Cecchin, M. G. Walker, R. S. Mulla, G. Battaglia, C. Smythe, J. A. Thomas, *Chem. Sci.* **2013**, *4*, 4512-4519.
- [48] A. Basu, S. Krishnamurthy, *J. Nucleic Acids* **2010**, *2010*, Article ID 201367.
- [49] G. He, J. Kuang, Z. Huang, J. Koomen, R. Kobayashi, A. R. Khokhar, Z. H. Siddik, *Br. J. Cancer* **2006**, *95*, 1514-1524.
- [50] A. Besson, S. F. Dowdy, J. M. Roberts, *Dev. Cell* **2008**, *14*, 159-169.
- [51] L. P. Martin, T. C. Hamilton, R. J. Schilder, *Clin. Cancer Res.* **2008**, *14*, 1291-1295.
- [52] I. M. Chu, L. Hengst, J. M. Slingerland, *Nat. Rev. Cancer* **2008**, *8*, 253-267.
- [53] F. M. Yakes, W. Chinratanalab, C. A. Ritter, W. King, S. Seelig, C. L. Arteaga, *Cancer Res.* **2002**, *62*, 4132-4141.
- [54] T. E. Miller, K. Ghoshal, B. Ramaswamy, S. Roy, J. Datta, C. L. Shapiro, S. Jacob, S. Majumder, *J. Biol. Chem.* **2008**, *283*, 29897-29903.
- [55] V. Guarneri, A. Frassoldati, A. Bottini, K. Cagossi, G. Bisagni, S. Sarti, A. Ravaioli, L. Cavanna, G. Giardina, A. Musolino, M. Untch, L. Orlando, F. Artioli, C. Boni, D. G. Generali, P. Serra, M. Bagnalasta, L. Marini, F. Piacentini, R. D'Amico, P. Conte, *J. Clin. Oncol.* **2012**, *30*, 1989-1995.
- [56] S. K. Karnik, C. M. Hughes, X. Gu, O. Rozenblatt-Rosen, G. W. McLean, Y. Xiong, M. Meyerson, S. K. Kim, *Proc. Natl. Acad. Sci. U. S. A.* **2005**, *102*, 14659-14664.

FULL PAPER

A binuclear ruthenium(II)-platinum(II) terpyridyl complex, VR54, inhibits cancer cell proliferation. In contrast to the vast majority of metal anticancer agents, VR54 is cytostatic and acts via up-regulating p27^{KIP1}, inhibiting Rb phosphorylation and inducing G1 cell cycle arrest.



Vadde Ramu, Martin R. Gill, Paul Jarman, David Turton, Jim A. Thomas,* Amitava Das* and Carl Smythe*

Page No. – Page No.

A cytostatic anticancer ruthenium(II)-platinum(II) bis(terpyridyl) anticancer complex that blocks entry into S phase by up-regulating p27^{KIP1}